Hydrological modeling in a highly urbanized watershed using explainable machine learning and sub-hourly data: A case study in the city of Sao Paulo, Brazil

Fernando L. Saraiva Filho[1], Elton Vicente Escobar-Silva[2], Marcos G. Quiles[1], Diego H. Stalder[3], and Leonardo B. L. Santos[1,2]

[1]Federal University of São Paulo, Av. Cesare Lattes, 1201, 12247-014, São José dos Campos, SP, Brazil
[2]National Center for Monitoring and Early Warning of Natural Disasters, Estrada Dr. Altino Bondensan, 500, 12247-016, São José dos Campos, SP, Brazil
[3]National University of Asunción, Engineering Faculty, San Lorenzo, Paraguay

Key Points:

- An appropriate selection of input data sources is crucial in a hydrological modeling scenario with non-continuous data.
- Ensemble models perform well in hourly hydrological modeling with forecasting horizons of up to 3 hours, with CatBoost standing out.
- SHAP values reveal insightful aspects of spatial and temporal dynamics of the rainfall-runoff relationship.

Corresponding author: Leonardo B. L. Santos, `santoslbl@gmail.com`

Abstract

Hydrological modeling of urbanized watersheds is a highly challenging task due to the complexity and non-linearity of the rainfall-runoff relationship in these areas. Many data-driven models have been proposed in the literature to address this problem. However, in this field, there is a need not only for performance but also for explainability and comprehension of the impacts of hydrometeorological factors. This study proposes a detailed comparative analysis between ensemble machine learning models using an explainable framework. We explore feature engineering and feature selection techniques to determine the best set of predictors in a situation of non-continuous data, a common problem in real-world scenarios. Among the models analysed, CatBoost stood out as the best-performing algorithm for most cases, and, in general, all the ensemble algorithms achieved good performance for a forecasting horizon up to 3 hours. A study with SHAP values revealed insightful aspects of the spatial and temporal dynamics of the rainfall-runoff relationship.

Plain Language Summary

Forecasting river levels in urban centers is a critical task in flood management. However, due to the complexities of these watersheds and the strong human intervention, this is a very challenging task, even more so if we consider that in many scenarios, it is not enough to have a good model. Still, it is also necessary to have an explainable model, that is, one that enables us to understand the impacts of different hydrometeorological factors. We proposed a comprehensive comparative study of state-of-the-art models associated with an explainability framework. We found that machine learning models based on the ensemble of simpler models can perform very well in this task, achieving good performance in forecasting horizons up to 3 hours. Furthermore, by employing appropriate techniques, it is possible to find valuable insights into the relation between precipitation in different coordinates and the variation of the river level. Finally, in scenarios where long periods go without data for specific stations, it is essential to make appropriate choices about which stations will be used in the modeling.

1 Introduction

Flash floods frequently cause many social and humanlosses in urban centers worldwide (Georgakakos et al., 2022), such as chaotic traffic, damage to buildings, economic losses, and deaths (Dharmarathne et al., 2024). Thus, forecasting river stage is a crucial tool for decision-makers.

There are several examples of hydrological models based on physical processes, e.g. (Arnold & Fohrer, 2005; Fernández-Pato et al., 2016). For any watershed, a process such as streamflow is affected by many physical characteristics (Pereira Filho & dos Santos, 2006). However, hydrological modeling of urbanized watersheds is a highly complex task because they are very heterogeneous and have specific hydrological processes (Salvadore et al., 2015). Furthermore, due to the high non-linearity and fluctuation of the rainfall-runoff relationship in these areas, developing a hydrological model for such areas with rapid response and good forecast performance is a challenging task (Cui et al., 2021).

Machine learning (ML) techniques have been widely applied to hydrological modeling (e.g. (Yaseen et al., 2015; Lange & Sippel, 2020; Mosaffa et al., 2022). On the other hand, these techniques do not take directly into account the physical processes involved but only seek to find relationships between inputs and outputs, explainability and physical consistency are challenges associated with the use of these approaches (Bhasme & Bhatia, 2024). Hence, ML algorithms are frequently criticized for their lack of explainability. Understanding the relative impacts of hydrometeorological factors is essential and could help authorities make better-informed decisions.

Given the foregoing, we propose a data-driven hydrological modeling based on machine learning techniques. Unlike traditional models, for which the role of data is secondary, being used only for calibration purposes, in data-driven models, the data entirely determines the proposed model (Szczepanek, 2022). We compare four tree-based ensemble ML models: Random Forest, XGBoost, LightGBM, and CatBoost. In this study, we apply SHAP (Lundberg & Lee, 2017), a powerful explainability technique, in conjunction with the ML models to quantify the effect of hydrometeorological factors on river-level (stage) forecasting at different lead times. Furthermore, we seek to support that a technique such as SHAP can be used to improve the explainability of black-box models for streamflow prediction, and this might be useful to persuade hydrologic modelers to utilize data-driven machine learning models with more confidence. Lastly, to the best of our knowledge, this is the first study to directly compare these models for the hourly forecasting of river level in an urbanized basin.

2 Materials and Methods

2.1 The study area

The area of interest of this work is the Tamanduateí River Watershed, which is within the São Paulo Metropolitan Area, Brazil, shown in Figure 1. This extremely urbanized watershed has a drainage area of 330.41 km^2 and covers the municipalities of Santo André, São Bernardo, São Caetano, Mauá, Diadema, and São Paulo. Tamanduateí River is 36.5 km long, rising in Mauá and flowing into Tietê River by a narrow-rectified channel (Gouveia & Rodrigues, 2017; Escobar-Silva et al., 2023). This watershed presents a time of concentration of about 3h50min, according to Kirpich's equation (Kirpich, 1940) considering an adaption for predominantly asphalted watersheds (Silveira, 2005). Furthermore, it has several records of floods, which greatly damage factories and residents of this region (Escobar-Silva et al., 2023; Tomás et al., 2022).

2.2 Data set and preprocessing

In this work, we use data from the Alto Tietê Telemetry Network, which is composed of a set of river stage and rainfall precipitation sensors. We obtain the data from the website of DAEE (DAEE, 2023). The first quarter of each year (from January to March) is one of the most rainy periods. For this reason, we focus our study on this period. We collect the data of the first quarters of 2018, 2019, 2020, 2021, and 2022. The data from 2018 and 2019 are used to train our models, whereas those from 2020 are used for validation. In the second step, the data from 2020 is integrated into the training dataset, and the data from 2021 and 2022 are used for tests. The temporal resolution of the data is 10 minutes.

Initially, there were 21 rain gauge stations and 15 stage gauge stations, which can be found in Table S1 and Table S2 (Supporting Information S1). However, due to missing values and data quality issues, some stations were removed before the modeling process, and only 10 rain gauge stations and 8 stage gauge stations are left, as can be found in Table S3 (Supporting Information S1). More details about the selection of the stations and the data cleaning process can be found in Text S1 (Supporting Information S1).

In order to tackle a time series forecasting problem using the supervised learning paradigm, it is necessary to use the embedding operation, which transforms the time series into a trajectory matrix (Takens, 2006), so that we can turn lagged versions of the time series into new inputs for the algorithms, creating what we call lag features. Therefore, we also use this technique in our work (for more information, see Text S2 in Supporting Information S1).

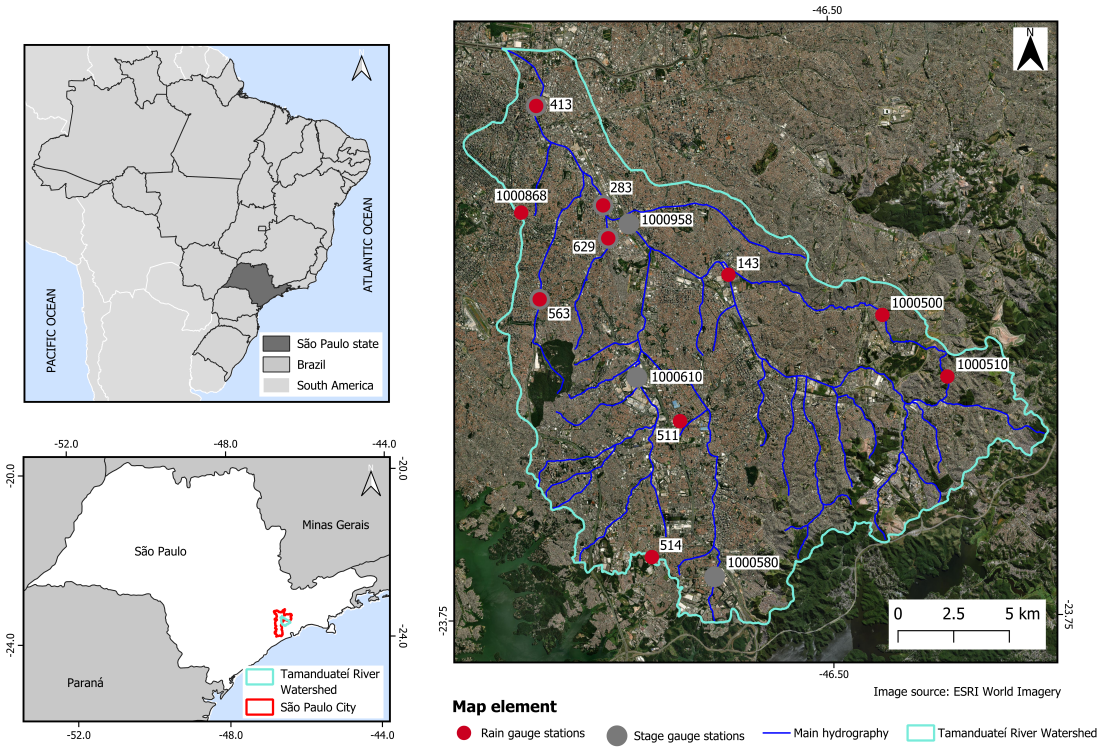

Figure 1: The spatial distribution of the rain and stage gauge stations within the Tamanduateí River Watershed, São Paulo, Brazil.

2.3 Ensemble algorithms

Random Forest is an ensemble algorithm that is built upon the concept of bagging/bootstrap aggregating (Breiman, 1996, 2001; Lee et al., 2020). The Gradient boosting algorithm was proposed by (Friedman, 2001) and is based on the combination of two main ideas: *Boosting* and *Gradient Descent*. The main idea of boosting is to add models sequentially so that, at each iteration, a new base learner is trained with respect to the error of the entire process learned so far (Natekin & Knoll, 2013). Extreme Gradient Boosting (XGBoost) is a scalable end-to-end implementation of Gradient boosting, and some of the main improvements brought by this implementation were a sparsity-aware algorithm for sparse data and weighted quantile sketch for approximate tree learning (Chen & Guestrin, 2016). Light Gradient Boosting Machine (LightGBM) also implements Gradient boosting and some variants, focusing on creating a computationally efficient algorithm (Ke et al., 2017). Categorical Boosting (CatBoost) stands for Categorical Boosting and is another implementation of Gradient boosting. One of its main goals is to tackle the problem originally named *prediction shift* (Prokhorenkova et al., 2018). For more details about Random Forest, Gradient Boosting, XGBoost, LightGBM, and CatBoost, see Text S3 in Supporting Information S1.

2.4 Evaluation metrics

Two metrics are used to evaluate the prediction performance of the proposed machine learning approach. The first is the Nash-Sutcliffe efficiency (NSE) (Nash & Sutcliffe, 1970). In hydrology, NSE is a widely used statistical measure that evaluates the performance of hydrological models, considering the model's estimation error relative to the mean of the observed data (Santos et al., 2023). It is defined by:

$$\mathrm{NSE} = 1 - \frac{\sum_{t=1}^{T}(y_t - Y_t)^2}{\sum_{t=1}^{T}(Y_t - \bar{Y})} \tag{1}$$

where T is the total number of time steps, y_t is the predicted river level at time t, Y_t is the observed river level at time t and $\bar{Y}$ is the observer water level mean. This index can range from $-\infty$ to 1, with 1 indicating a perfect prediction.

The second metric that we use is the very famous Root Mean Squared Error (RMSE):

$$\mathrm{RMSE} = \sqrt{\frac{\sum_{t=1}^{T}(Y_t - y_t)^2}{T}} \tag{2}$$

2.5 Feature engineering and feature selection

The primary feature engineering technique is the time-delay embedding previously described, which is used to transform the time series structure into a matrix structure. Furthermore, in order to select the best set of lag features, we use the Autocorrelation Function (ACF) and the Partial Autocorrelation Function (PACF), as time series sometimes have linear relations with lagged versions of itself (for details, see Text S4 in Supporting Information S1). We also use a technique called Recursive Feature Elimination (RFE), which is based on an iterative process of training the algorithm, computing the importance of the input features, and eliminating the least important ones (Guyon et al., 2002).

2.6 SHAP

The explainability of ML models using SHapley Additive exPlanations (SHAP) in hydrology modeling has emerged as an alternative to solve this issue. SHAP is a game

theory framework that can analyze the interaction of characteristics and provide the relative contribution of each characteristic to the target variables (Lundberg & Lee, 2017). By integrating SHAP into the models, it is possible to obtain estimates of the contribution of each input feature in the determination of the prediction, and local interpretations are provided through the generation of perturbations of a given instance of the dataset (Fan et al., 2023). Therefore, SHAP can be called an instance-based explainer because it calculates feature contributions for each prediction, and can provide explanations on a global level by combining the local ones (Lundberg et al., 2019).

2.7 Experiments

In developing an ML modeling process, choosing of the set of input features is a crucial step. Therefore, to forecast the river level at the outlet of the watershed, we initially explored the influence of different physical variables, comparing the forecasting performance in different experiments that use different input sets. The set of experiments is defined as $E = \{e_1, e_2, e_3, ..., e_7\}$. The set of rain gauges fixed as $R = \{R_1, R_2, ..., R_{10}\}$ and R_1 is the rain gauge located in the Mercado Municipal (Station ID 413), the point near the watershed outlet (pour point), which is the target of the forecasting. The set of hydrological stations is $H = \{H_1, H_2, ..., H_7\}$, and H_1 is the hydrological station located in the Mercado Municipal (Station ID 413). Next, we describe the set of inputs used in each experiment. In e_1, only the rain gauge at the outlet; in e_2, all the rain gauges; in e_3, only the hydro station at the outlet; in e_4, the rain gauge and the hydro station at the outlet; in e_5, all the rain gauges and the hydro station at the outlet; in e_6, all the hydro stations, and in e_7, all the rain gauges and all the hydro stations.

In this first comparison, we use Random Forest and the input is only the current data at time t of the sensors. The output is the river level at the outlet two hours ahead. We use the validation data of 2020 to optimize the hyperparameters of the algorithm in each of the seven experiments. The optimization uses the open-source library Optuna, which employs Bayesian optimization. Further details about Optuna can be found in (Akiba et al., 2019). For each of the seven experiments, we run 50 trials with Optuna, considering the range of hyperparameters in Table S4 (Supporting Information S1). After obtaining the optimized hyperparameters, we assimilate the data from 2020 in the training data set and we use the data from 2021 and 2022 as a test dataset, and make the comparison between the seven situations once. After determining the best set of physical input features, we use the time delay embedding strategy to build new lag features and assess the performance improvement that their use brings.

Then, we compare the performance of different ensemble-based machine learning algorithms (Random Forest, XGBoost, LightGBM, and CatBoost). We compare their performance for various forecasting lead times to determine to what extent we could achieve good predictions. We then apply a feature selection technique, and finally, we use the SHAP values to analyze the explainability of the models, exploring spatial-temporal relationships between stations.

3 Results and Discussion

3.1 Selection of stations

Using Random Forest, we compare the seven experiments with different sets of stations as inputs, as explained in Section 2.7. In Supporting Information S1, we present all the results for the seven experiments for the validation dataset (2020) in Table S5, and in Table S6, we present the results for the test dataset (2021+2022). In Table S5, in particular, it is interesting to notice that the optimization of the hyperparameters improved the forecasting performance in all situations, with the improvement in RMSE reach-

ing more than 4% in experiments e_3, e_5, e_6. The RMSE and NSE for all these experiments can also be seen in Figure S3 in Supporting Information S1.

The best performance in the training dataset is achieved in e_7, i.e., the experiment that presents the largest amount of information being used as inputs (all rain gauge stations and all stage gauge stations), as shown in Figure S3 in Supporting Information S1. However, it is interesting to notice that for the validation set, the best performance is achieved in e_5, the experiment that uses all the rain gauge stations and only the stage gauge at the outlet as inputs.

Furthermore, experiment e_6, the one that uses as inputs all the stage gauge stations but does not use any rain gauge station, presents a very high performance in the training dataset with $NSE = 0.889$ but very low performance in the test data set with $NSE = 0.293$ as can be seen in Figure S3 and Table S6 in Supporting Information S1. Therefore, we note that using data from other hydrological stations causes the model to perform very well in the training dataset but poorly in the test dataset. A first assumption could be that, over the years, the distributions of the time series of the river level at different stations have changed, representing a drift that is not learned in the modeling process. This hypothesis can be validated with the Kolmogorov-Smirnov test, which checks whether different sets of data follow the same distribution (for more details, see Text S5 in Supporting Information S1). The p-values for the Kolmogorov-Smirnov test between versions of the timeseries of each station for different years are shown in Table S7 (Supporting Information S1). For the rain gauge stations, most p-values are higher than 0.05, indicating that the values follow the same distribution in different years. However, for stage gauge stations, all p-values are less than 0.05, providing evidence that the distribution of the measured values in a stage gauge station undergoes significant change between the first quarter of one year and the next. In Figure S3 (Supporting Information S1), it is possible to see that, for the target station, for example, the distribution of the river is distinct between different years. Possible explanations for that are human intervention in the watershed or new calibrations of the sensors through the years.

This evidence points to the conclusion that, in urbanized basins, in situations where the training data is composed of intermittent periods, with spacings of months, for example, the most efficient approach is to use only the rain gauges and the memory itself of the target hydrological station, foregoing the use of other hydrological stations. From this point onwards in our work, all analyses refer to this set of inputs from the experiment e_5.

In Text S7 in Supporting Information, we present a discussion about how the use of lags of the time series ranging from $t - 0$ to $t - 13$. By using the lags and optimizing the hyperparameters, we obtain an improvement in performance for the test dataset, as the NSE increases from 0.714 to 0.756 and the RMSE decreases from 45.3 cm to 41.8 cm when we use lag features. The improvement represents a decrease of approximately 7.7% in the RMSE. This confirms the usefulness of the lag features in our forecasting problem.

3.2 Comparison of different ML models

Regarding the comparison of the performance of the RF with more modern ensemble-based algorithms (XGBoost, LightGBM, and CatBoost), we also compare their forecasting performance to that of Naive Persistence as a baseline. This baseline algorithm assumes that the future value is equal to the last measured value. This comparison is conducted not only for the forecasting horizon of 2 hours but for all integer values ranging from 1 hour to 8 hours. The results are presented in Table S8 (Supporting Information S1) and can be visualized in Figure 2. In Figure 2, excerpts of the stage hydrogram illustrate the observed and predicted values for different algorithms for the 2-hour ahead forecasting.

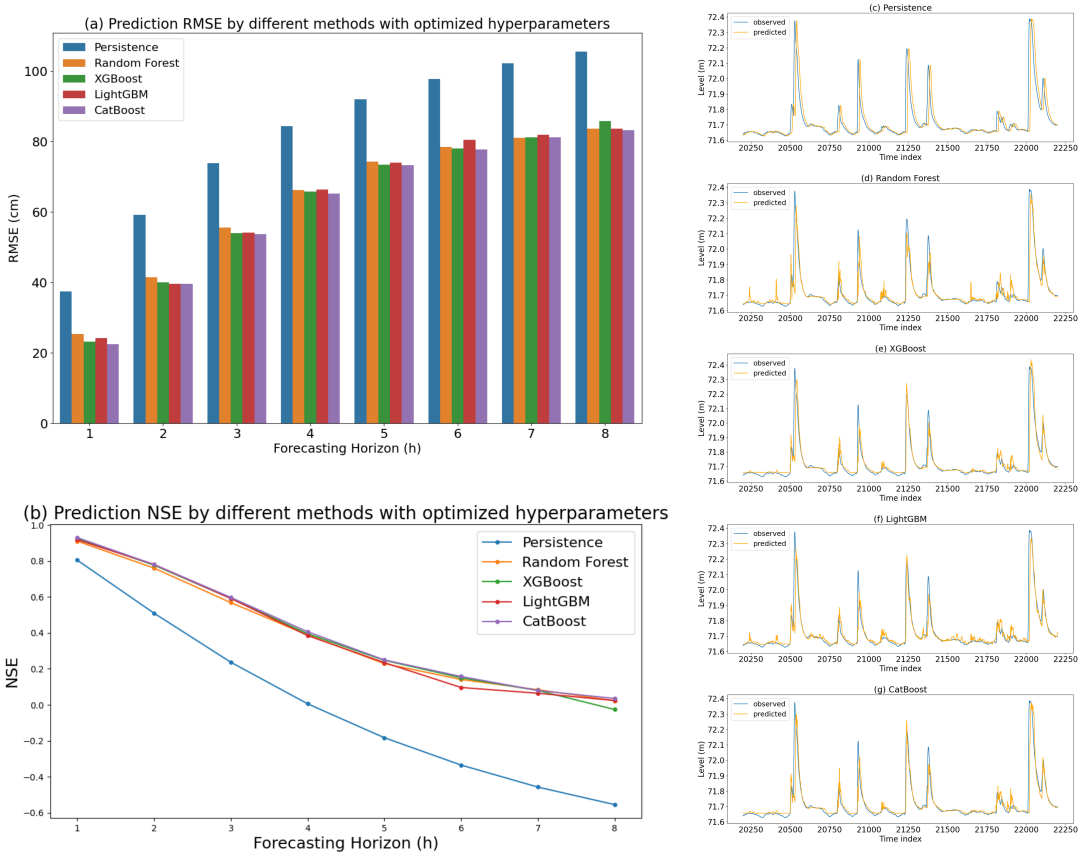

Figure 2: Comparison of the performance of the different algorithms for different forecasting horizons. (a) Comparison of RMSE. (b) Comparison of NSE. The other charts are excerpts from the stage hydrograms using (c) Persistence, (d) Random Forest, (e) XGBoost, (f) LightGBM, (g) CatBoost.

The performances of all the ensemble algorithms are similar and significantly better than Persistence, the baseline (Figure 2 and Table S6). Furthermore, considering the eight different forecasting horizons, CatBoost achieved the best performance in seven of them, in terms of RMSE and NSE. It did not achieve the best performance only for the horizon 7. XGBoost also presents a very good performance and achieves the best or the second-best performance in five out of the eight cases. On the other hand, RF presents a slightly worse performance, achieving the lowest performance among the ensemble algorithms in five out of the eight cases. However, in general, all the ensemble algorithms achieve similar performance in these experiments. In the case of the 4-hour forecasting horizon, we have the following values of RMSE: Random Forest achieves 66.2 cm, XGBoost 65.8 cm, LightGBM 66.4 cm, and CatBoost 65.2 cm. Therefore, even though CatBoost has the best performance and Random Forest has the worst one among the ensemble algorithms, the difference between the best and the worst is less than 1.6%.

For longer lead times, the forecasting performance becomes worse. For the lead time of 1 hour, we achieve excellent performance, with all the ensemble algorithms achieving NSE values higher than 0.9. In the 2 hours ahead forecasting, all the ensemble algorithms achieve good performance, having values of NSE higher than 0.76. In the case of the 3-hour forecasting horizon, the performance of the algorithms is reasonable, and the values of NSE are between 0.56 and 0.60. From the 4-hour case onwards, the algorithms achieve poor forecasting performance, and all NSE values are less than 0.41.

3.3 Feature Selection

Among the various benefits that feature selection offers in an ML modeling process, one key advantage is improving the explainability of the models. From Figure S3 in Supporting Information S1, we observe that the previous lags of our target station's time series are highly correlated. Therefore, we perform feature selection to identify only the most informative lags. In the previous section, we utilized all the lags from our target station, ranging from $t-13$ to $t-0$. Now, we apply the RFE approach with Random Forest to extract just the three most significant lags of the river level time series.

Applying RFE, in the case of the 1-hour forecasting horizon, we find that the most important lags are $t-0$, $t-2$, and $t-3$. Using all the same rain gauge lags used before, but only these lags of the river level, we achieve even better performance than in the case in which we used all lags of the river level. In the case of the 2-hour forecasting horizon, the most important lags are $t-0$, $t-2$, and $t-13$, and in the case of a 3-hour horizon, the most important ones are $t-0$, $t-4$, and $t-13$. In both cases, the new metrics are better or approximately equal to the ones in the case without feature selection (see Text S6 in Supporting Information S1). We also analyze a new forecasting horizon: 30 minutes. For this horizon, the best lags are $t-0$, $t-2$, and $t-3$.

3.4 Explainability

In this section, we present and discuss the Shapley values obtained from the two algorithms that achieved the best performance: XGBoost and CatBoost. These values can be seen in Figure 3 for various lead times. In every case, the river level memory is crucial for forecasting in general, surpassing the significance of all rain gauges (Figure 3).

For the 30-minute forecasting horizon, the most important rain gauge is 413 at lag $t-0$ for XGBoost, and it is also quite significant for CatBoost, being its second-most-important rain gauge feature. This is physically reasonable, as rain gauge 413 collects data on rainfall from the area near the outlet, which is evidently the most crucial information for forecasting over such a short period. It is also noteworthy that, for CatBoost, while the second most important rain gauge feature is 413 at lag $t-0$, the top feature

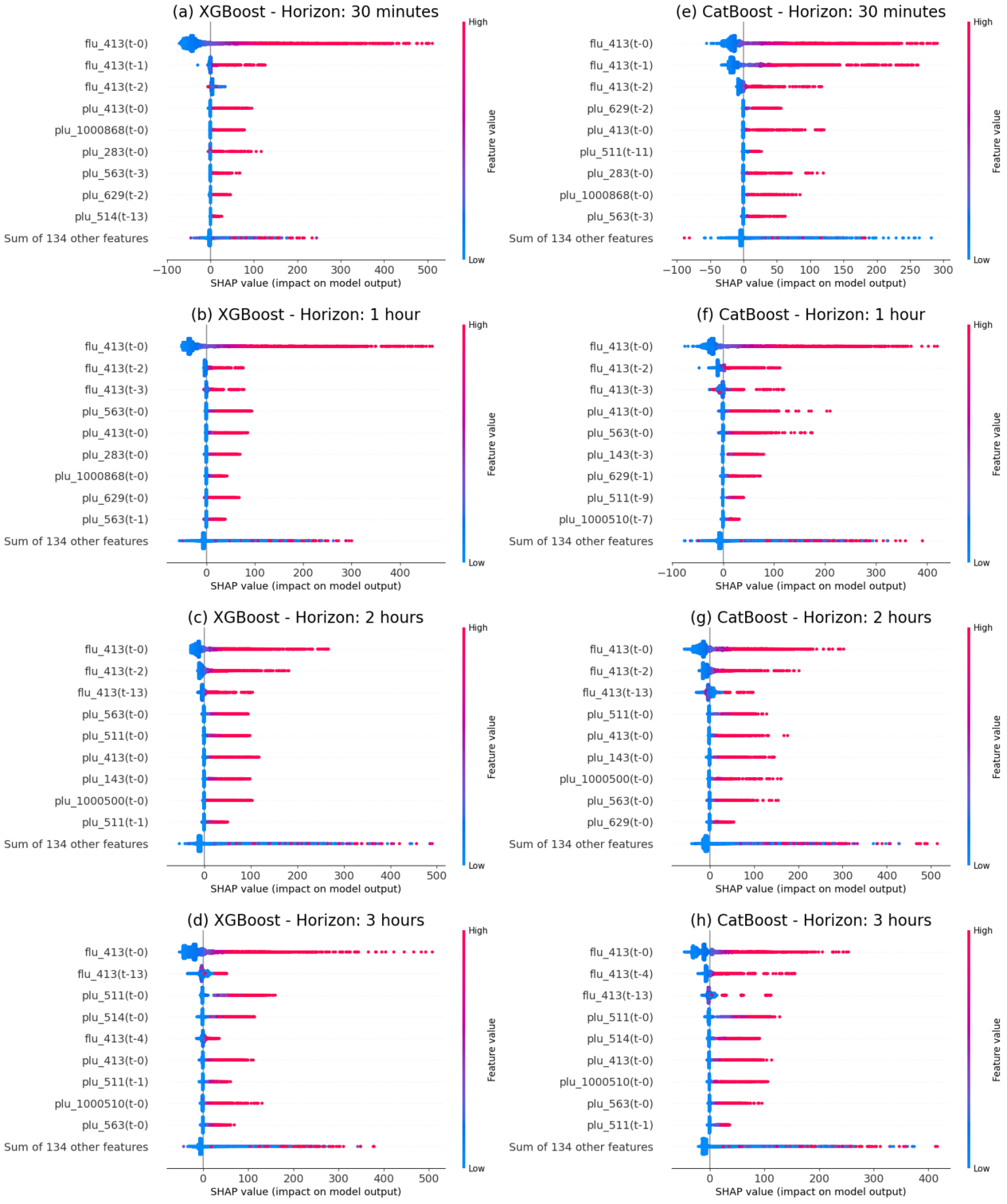

Figure 3: Shapely values for the test dataset obtained with XGBoost and CatBoost for different forecasting horizons.

is 629 at lag $t-2$. Given that rain gauge 629 is one of the closest stations to the outlet, its relevance is expected, though the importance at lag $t-0$ is diminished since water takes time to travel from station 629 to the outlet. Additionally, for CatBoost, the third most important rain feature is rain gauge 511 at lag $t-11$. This longer time lag reflects the greater geographical distance from the station to the outlet, indicating that water requires more time to reach its destination.

For the 1-hour horizon, the most significant rain gauge for XGBoost is no longer 413, while rain gauge 563 increases in significance. This is physically understandable because rain gauge 563 is located a bit further from the outlet, making the rainfall in its vicinity more relevant for forecasting the river at the outlet within the 1-hour horizon. Nevertheless, rain gauge 413 remains important, ranking second most significant. In contrast, for CatBoost, the importance of these two features is reversed compared to XGBoost. For the 2-hour horizon, the rain gauge 511 at lag $t-0$ becomes more relevant, being the most important rain feature for CatBoost and the second most important rain feature for XGBoost. However, the rain gauge 511 did not play such an important role when we considered the 1-hour horizon. As the lead time increases, it is very interesting to notice how further stations become more relevant, which is totally physically consistent, considering the time that the water takes to travel between these points.

For the 3-hour horizon, a new rain gauge gains prominence for both algorithms: the rain gauge 514 at lag $t-0$. This is a new evidence of physical consistency, as it shows that the longer the forecasting horizon, the greater the importance of rain gauges that are further away from the outlet. It is also remarkable that station 514 gains such high importance when the forecasting horizon is 3 hours because this station is near the border of the watershed, and the time the water takes to travel from this point to the outlet should be a value near the concentration time of the basin, which is indeed what happens. We do not expect these numbers to match perfectly as the rain gauges represent a punctual measurement of rainfall distributed across a region.

By examining SHAP values over different forecasting horizons and algorithms, we obtain a clearer insight into how predictions are formed and how the significance of features corresponds with reality from both spatial and temporal viewpoints.

4 Conclusions and future work

This study developed an explainable machine learning framework to predict hourly river levels in an urban watershed. The evaluation of ensemble-based methods demonstrated that all algorithms significantly outperformed Persistence across forecasting horizons ranging from 1 to 8 hours. For shorter lead times, all ensemble algorithms exhibited excellent performance, with NSE values exceeding 0.9 for the 1-hour horizon. CatBoost consistently delivered the best results, securing the best performance for seven out of eight forecasting horizons. Meanwhile, RF showed the weakest performance among the ensemble algorithms. However performance differences were generally minimal, with less than a 1.6% difference in RMSE for the 4-hour forecasting horizon, for example. Furthermore, as expected, the performance of the algorithms gradually declined with longer lead times, so we obtained satisfactory forecasting performance only up to 3-hour lead time.

The incorporation of SHAP analysis yielded valuable insights into the spatial and temporal dynamics influencing model predictions, revealing how lagged river level and precipitation measurements play different roles depending on the forecasting horizon. SHAP results demonstrated that ML models make predictions physically consistent, assigning more importance to stations nearer to the outlet when the forecasting horizon is shorter and to stations further to the outlet when the forecasting horizon is longer. Therefore, for short-term horizons, the local precipitation dominates the model's predictions, while

upstream rainfall gains more importance for long-term horizon. These findings emphasize the necessity of incorporating spatio-temporal factors into flood simulation methodologies.

Evidence suggests that when training data is non-continuous, a prevalent situation in practical cases, using only rain gauges and the corresponding stage gauge station as inputs is the most effective strategy. This is especially crucial in settings with considerable human involvement, where the interrelations among variables might fluctuate dramatically with the seasons, and in real-world scenarios, where sensor malfunctions or connectivity issues often occur.

This research enhances confidence in hydrological forecasting by transforming ensemble ML models from opaque predictors into explainable tools. The insights gained in this work can help decision-makers improve urban flood risk management and emergency response strategies, thus fostering more resilient urban infrastructure. Future research will expand this framework to include additional input sources, like radar, to improve the performance for longer lead times, and explore new ML architectures and explainability techniques, advancing the field of explainable hydrological modeling.

Open Research Section

The source code and data supporting this letter are publicly available in a GitHub repository, allowing other researchers to replicate the case study presented here. The code can be accessed at https://doi.org/10.5281/zenodo.14968431.

Acknowledgments

This study was financed by the Coordination for the Improvement of Higher Education Personnel (CAPES), Finance Code 001 (F.L.S.F.), by the São Paulo Research Foundation (FAPESP), grant nº. 2024/02748-7 (E.V.E.S.), and by the Brazilian National Council for Scientific and Technological Development (CNPq), grant nº. 446053/2023-6 (L.B.L.S.). Lastly, the authors thank the Brazilian Ministry of Science, Technology, and Innovation and the Brazilian Space Agency.

References

Akiba, T., Sano, S., Yanase, T., Ohta, T., & Koyama, M. (2019). Optuna: A next-generation hyperparameter optimization framework. In *Proceedings of the 25th acm sigkdd international conference on knowledge discovery & data mining* (p. 2623–2631). New York, NY, USA: Association for Computing Machinery. Retrieved from `https://doi-org.ez69.periodicos.capes.gov.br/10.1145/3292500.3330701` doi: 10.1145/3292500.3330701

Arnold, J. G., & Fohrer, N. (2005). Swat2000: current capabilities and research opportunities in applied watershed modelling. *Hydrological Processes*, *19*(3), 563-572. Retrieved from `https://onlinelibrary.wiley.com/doi/abs/10.1002/hyp.5611` doi: https://doi.org/10.1002/hyp.5611

Bhasme, P., & Bhatia, U. (2024). Improving the interpretability and predictive power of hydrological models: Applications for daily streamflow in managed and unmanaged catchments. *Journal of Hydrology*, *628*, 130421.

Breiman, L. (1996). Bagging predictors. *Machine learning*, *24*, 123–140.

Breiman, L. (2001). Random forests. *Machine learning*, *45*, 5–32.

Chen, T., & Guestrin, C. (2016). Xgboost: A scalable tree boosting system. In *Proceedings of the 22nd acm sigkdd international conference on knowledge discovery and data mining* (pp. 785–794).

Cui, Z., Qing, X., Chai, H., Yang, S., Zhu, Y., & Wang, F. (2021). Real-time rainfall-runoff prediction using light gradient boosting machine coupled with

singular spectrum analysis. *Journal of Hydrology*, *603*, 127124.

DAEE. (2023). Retrieved from `http://sibh.daee.sp.gov.br/`

Dharmarathne, G., Waduge, A., Bogahawaththa, M., Rathnayake, U., & Meddage, D. (2024). Adapting cities to the surge: A comprehensive review of climate-induced urban flooding. *Results in Engineering*, 102123.

Escobar-Silva, E. V., Almeida, C. M. d., Silva, G. B. L. d., Bursteinas, I., Rocha Filho, K. L. d., de Oliveira, C. G., ... Paiva, R. C. D. d. (2023). Assessing the extent of flood-prone areas in a south-american megacity using different high resolution dtms. *Water*, *15*(6), 1127.

Fan, M., Zhang, L., Liu, S., Yang, T., & Lu, D. (2023). Investigation of hydrometeorological influences on reservoir releases using explainable machine learning methods. *Frontiers in Water*, *5*, 1112970.

Fernández-Pato, J., Caviedes-Voullième, D., & García-Navarro, P. (2016). Rainfall/runoff simulation with 2d full shallow water equations: Sensitivity analysis and calibration of infiltration parameters. *Journal of Hydrology*, *536*, 496-513. Retrieved from `https://www.sciencedirect.com/science/article/pii/S0022169416301263` doi: https://doi.org/10.1016/j.jhydrol.2016.03.021

Friedman, J. H. (2001). Greedy function approximation: A gradient boosting machine. *The Annals of Statistics*, *29*(5), 1189 – 1232. Retrieved from `https://doi.org/10.1214/aos/1013203451` doi: 10.1214/aos/1013203451

Georgakakos, K. P., Modrick, T. M., Shamir, E., Campbell, R., Cheng, Z., Jubach, R., ... Banks, R. (2022). The flash flood guidance system implementation worldwide: A successful multidecadal research-to-operations effort. *Bulletin of the American Meteorological Society*, *103*(3), E665–E679.

Gouveia, I. C. M.-C., & Rodrigues, C. (2017). Mudanças morfológicas e efeitos hidrodinâmicos do processo de urbanização na bacia hidrográfica do rio tamanduateí–rmsp. *GEOUSP Espaço e Tempo (Online)*, *21*(1), 257–283.

Guyon, I., Weston, J., Barnhill, S., & Vapnik, V. (2002). Gene selection for cancer classification using support vector machines. *Machine learning*, *46*, 389–422.

Ke, G., Meng, Q., Finley, T., Wang, T., Chen, W., Ma, W., ... Liu, T.-Y. (2017). Lightgbm: A highly efficient gradient boosting decision tree. *Advances in neural information processing systems*, *30*.

Kirpich, Z. (1940). Time of concentration of small agricultural watersheds. *Civil engineering*, *10*(6), 362.

Lange, H., & Sippel, S. (2020). Machine learning applications in hydrology. *Forest-water interactions*, 233–257.

Lee, T.-H., Ullah, A., & Wang, R. (2020). Bootstrap aggregating and random forest. *Macroeconomic forecasting in the era of big data: Theory and practice*, 389–429.

Lundberg, S. M., Erion, G., Chen, H., DeGrave, A., Prutkin, J. M., Nair, B., ... Lee, S.-I. (2019). Explainable ai for trees: From local explanations to global understanding. *arXiv preprint arXiv:1905.04610*.

Lundberg, S. M., & Lee, S.-I. (2017). A unified approach to interpreting model predictions. *Advances in neural information processing systems*, *30*.

Mosaffa, H., Sadeghi, M., Mallakpour, I., Jahromi, M. N., & Pourghasemi, H. R. (2022). Application of machine learning algorithms in hydrology. In *Computers in earth and environmental sciences* (pp. 585–591). Elsevier.

Nash, J., & Sutcliffe, J. (1970). River flow forecasting through conceptual models part i — a discussion of principles. *Journal of Hydrology*, *10*(3), 282-290. Retrieved from `https://www.sciencedirect.com/science/article/pii/0022169470902556` doi: https://doi.org/10.1016/0022-1694(70)90255-6

Natekin, A., & Knoll, A. (2013). Gradient boosting machines, a tutorial. *Frontiers in Neurorobotics*, *7*. Retrieved from `https://www.frontiersin.org/journals/neurorobotics/articles/10.3389/fnbot.2013.00021` doi: 10.3389/fnbot.2013.00021

Pereira Filho, A. J., & dos Santos, C. C. (2006). Modeling a densely urbanized watershed with an artificial neural network, weather radar and telemetric data. *Journal of Hydrology*, *317*(1), 31-48. Retrieved from https://www.sciencedirect.com/science/article/pii/S0022169405002593 doi: https://doi.org/10.1016/j.jhydrol.2005.05.007

Prokhorenkova, L., Gusev, G., Vorobev, A., Dorogush, A. V., & Gulin, A. (2018). Catboost: unbiased boosting with categorical features. In S. Bengio, H. Wallach, H. Larochelle, K. Grauman, N. Cesa-Bianchi, & R. Garnett (Eds.), *Advances in neural information processing systems* (Vol. 31). Curran Associates, Inc. Retrieved from https://proceedings.neurips.cc/paper/2018/file/14491b756b3a51daac41c24863285549-Paper.pdf

Salvadore, E., Bronders, J., & Batelaan, O. (2015). Hydrological modelling of urbanized catchments: A review and future directions. *Journal of hydrology*, *529*, 62–81.

Santos, L. B. L., Freitas, C. P., Bacelar, L., Soares, J. A. J. P., Diniz, M. M., Lima, G. R. T., & Stephany, S. (2023). A neural network-based hydrological model for very high-resolution forecasting using weather radar data. *Eng*, *4*(3), 1787–1796. Retrieved from https://www.mdpi.com/2673-4117/4/3/101 doi: 10.3390/eng4030101

Silveira, A. L. L. d. (2005). Performance of time of concentration formulas for urban and rural basins. *RBRH: Revista Brasileira de Recursos Hídricos. Porto Alegre, RS: ABRH. Vol. 10, n. 1 (jan./mar. 2005), p. 5-23*.

Szczepanek, R. (2022). Daily streamflow forecasting in mountainous catchment using xgboost, lightgbm and catboost. *Hydrology*, *9*(12), 226.

Takens, F. (2006). Detecting strange attractors in turbulence. In *Dynamical systems and turbulence, warwick 1980: proceedings of a symposium held at the university of warwick 1979/80* (pp. 366–381).

Tomás, L. R., Soares, G. G., Jorge, A. A., Mendes, J. F., Freitas, V. L., & Santos, L. B. (2022). Flood risk map from hydrological and mobility data: A case study in são paulo (brazil). *Transactions in GIS*, *26*(5), 2341–2365.

Yaseen, Z. M., El-Shafie, A., Jaafar, O., Afan, H. A., & Sayl, K. N. (2015). Artificial intelligence based models for stream-flow forecasting: 2000–2015. *Journal of Hydrology*, *530*, 829–844.